MRS Advances (2022) 7:668–673
https://doi.org/10.1557/s43580-022-00372-6

ORIGINAL PAPER

Carbon nanomaterials synthesis by chemical vapor deposition from conifer exudate

Juan Luis Ignacio-De la Cruz[1] · Carmen Judith Gutiérrez-García[2] · David Ricardo Poiré-De la Cruz[1] · María Remedios Cisneros-Magaña[1] · Orlando Hernández-Cristóbal[3] · Juan Manuel Sánchez-Yáñez[1] · Nelly Flores-Ramirez[1] · Lada Domratcheva-Lvova[1]

Received: 9 September 2022 / Accepted: 26 October 2022 / Published online: 8 November 2022

Abstract

Carbon nanostructures were synthesized using coniferous exudate commonly known as rosin as precursor due their high carbon content, low cost, and because it is a renewable material with high availability. The synthesis of the carbon nanostructures (CNSs) was carried out by the chemical vapor deposition (CVD) technique with a stainless steel AISI 304 bar as catalyst and argon as the carrier gas at 750, 800, 850, and 900 °C during 30 and 60 min at atmospheric pressure. The scanning electron microscopy demonstrated the formation of mostly spherical and some tubular carbon nanostructures of different diameters. The carbon spheres at higher temperatures are more defined; however, they tend to agglomerate. Energy-dispersive spectroscopy analysis demonstrated 84–99% of carbon, 0.25–15.69% of oxygen, and traces of chromium and iron. The Fourier transform infrared spectra indicated the presence of OH, C=O, C=C, and CH_x functional groups. The presence of hydroxyl and carbonyl groups can be useful for higher interaction of CNSs with different materials in some usage. Typical D, G, and G′ bands of CNSs were observed by Raman spectroscopy. The ID/IG ratio show high degree of graphitization of CNSs. The value of IG′/IG ratio indicates that the CNSs are multilayer. X-ray diffraction patterns show that the CNSs obtained at 30 min are more crystalline. The CNSs synthesized from rosin by CVD can be used in different fields of science and technology.

Introduction

Nanomaterials such as single and multiwalled nanotubes, graphene, fullerenes, microspheres and nanospheres, receive considerable attention due to their potential in a wide spectrum of applications such as nanoadditives, energy storage devices, nanotransistors, catalyst supports, and nanocomposites [1, 2].

Carbon nanomaterials synthesis commonly uses petrochemicals due their high carbon percentage; however, some of precursors possess toxicity and can cause damage to the environment [3, 4].

Each year about 1,300,000 tons of rosin is produced worldwide. The most part of production of rosin is concentrated in China, Brasil, and Indonesia. Mexico also produces and exports rosin. The rosin extraction in Mexico is mainly carried out in four states: Jalisco, Oaxaca, Mexico, and Michoacán, the latter one ranked first in the country with 22,408 tons per year, with 86.7% of the total national production [5]. The amounts available of rosin are high and this can be one of the reasons because the rosin can be an excellent green option for production of carbon nanomaterials and to scale the process. The high percentage of carbon, as well as a vapor pressure of 4.8–10.8 mbar, an evaporation temperature of 202 °C and the structure of compounds components of rosin are also the positive factors in choosing of rosin as green precursor for carbon nanostructures synthesis. The implementation of green chemistry principles seeks to minimize the indiscriminate use of petroleum derived hydrocarbons in the synthesis of carbon nanostructures, taking as a priority to preserve the environment and human health, proposing the use of green

✉ Lada Domratcheva-Lvova
ladamex@yahoo.es

[1] Universidad Michoacana de San Nicolás de Hidalgo, Av. Francisco J. Múgica S/N, Felicitas del Río, 58030 Morelia, Michoacán, Mexico

[2] División de Estudios de Posgrado e Investigación, Tecnológico Nacional México/Instituto Tecnológico de Morelia, Avenida Tecnológico 1500, 58120 Morelia, Michoacán, Mexico

[3] ENES, UNAM, Unidad Morelia, Antigua Carretera a Pátzcuaro 8701, 58190 Morelia, Mich., Mexico

resources as a sustainable and ecological alternative [6, 7]; furthermore, the green sources have the several advantages, such as low cost and availability [8]. Some research reports the successful use of renewable source in nanomaterial synthesis, such as rosins, camphor, and biomass [9, 10]. Chemical vapor deposition (CVD) is a simple method, is versatile with the use of different green carbon precursors, has relatively low cost, and one-step process in the nanomaterial's synthesis [11]. Moreover, the use of the metallic catalyst favors carbon nanomaterials growth optimizing the energy used in this method [12]. The objective of this research is to synthesize carbon nanomaterials from conifer exudate (rosin) as green precursor by CVD method with an AISI 304 stainless steel bar as catalyst.

Materials and methods

The nanomaterials were synthesized in a quartz reactor 60 cm × 2.54 cm length and diameter, respectively, using as the only carbon source 1.0 g of coniferous exudate for each experiment and an austenitic stainless steel bar (AISI 304) as catalyst with 10 mL/min of argon as carrier gas. The synthesis temperatures were 750, 800, 850, and 900 °C with reaction times 30 and 60 min at atmospheric pressure. Average heating rate in the furnace was 1.2 °C/s, while the average cooling rate was 0.12 °C/s; the synthesis proceed when target temperature of each experiment was achieved. The rosin evaporation temperature was 202 °C. The synthesized nanomaterials were characterized by Scanning Electron Microscopy SEM-JEOL JSM-IT300LV coupled with an energy-dispersive spectrometer (EDS), to determine their morphological structure and the elemental chemical composition of the nanomaterial. Fourier transform infrared spectroscopy (FTIR-TENSOR 27 Bruker) was used to detect the main functional groups involved in the formation of the nanomaterials from a green precursor, Raman spectroscopy (Thermo Scientific DXR) was used to obtain detailed information on the chemical structure, the graphitization degree, and evaluation of number of graphene layers of nanostructures. The intensities of the bands D, G, and G´ were measured. Then the ratio of intensities of D band with G band was calculated for determine the degree of graphitization. Also, the ratio of intensities of G′ with G band was evaluated for estimate layered numbers of graphene sheets in carbon spheres. X-Ray Diffraction (Bruker—D8 Advance) was useful to provide the crystalline identification of the nanomaterials synthesized. The diameter of nanomaterials was measured with ImageJ software. The measuring of 100 carbon spheres of each sample was realized. Then the calculation of the average for each temperature and reaction time was done.

Results and discussion

SEM micrographs demonstrated spherical and tubular shapes of obtained carbon nanomaterials (CNs), prevailing carbon spheres (CSs) at temperatures of 850 and 900 °C at 30 and 60 min. CNs diameter were 190–2000 nm for CSs and 120–180 nm for carbon nanotubes (CNTs). At 750 °C/30-min synthesis conditions, CSs with diameters less than 120 nm and CNTs with 140–180 nm were obtained (Fig. 1a). Some graphite dots could be observed on CSs obtained at 800 °C/30 min. These CSs, with diameters 650–830 nm, present agglomeration due to coalescence effects (Fig. 1b). At 850 °C/30 min, the growth of 775–1730 nm CSs was observed (Fig. 1c). At 900 °C/30 min, the only synthesis product were CSs with a size smaller than 265 nm. These CSs presented agglomeration due to coalescence effect (Fig. 1d). The micrographs of samples obtained at 750 °C/60 min demonstrated 770–1200-nm CSs (Fig. 1e). The CNs obtained at 800 °C/60 min are 600–900-nm CSs and CNTs with diameters less than 100 nm (Fig. 1f). The micrographs of samples obtained at 850 °C/60 min (Fig. 1g) and at 900 °C/60 min (Fig. 1h) demonstrated just the presence of CSs with diameters 350–495 nm and 260–375 nm, respectively. The results demonstrated that the CSs obtained at higher temperatures are more defined; however, they tend to agglomerate. This could be due to the fact that the CSs are attracted by Van der Waals forces, which leads to agglomeration [13]. The formation of carbon spheres according to the literature could be attributed to the presence of aromatic rings from coniferous exudates [14], which can be either pentagonal or heptagonal, which are necessary to modulate CSs curvature [15, 16]. The results of this research are similar to those reported by Ambriz-Torres, who produced CNs from two different precursors: naphthalene and rubber waste from tire by CVD at similar conditions. In the case of naphthalene precursor she obtained the carbon spheres and some quantity of carbon nanotubes; from rubber residues just CSs were produced. The diameters of carbon spheres obtained from both precursors are smaller than obtained in the present research [17]. Guzman-Fuentes synthesized CSs using cis-1,4-polyisoprene (natural rubber) as a green precursor under similar conditions of reported in the present paper [18]. Gutierrez-García reported just the formation of carbon spheres with comparable diameters from polynuclear aromatic precursors at similar conditions [19].

EDS analysis (Table 1) demonstrated that the predominant elements were carbon with 84 to 99% atomic, followed by the oxygen between 0.25 and 15%, both elements can be proceeded from the rosin precursor [9]. The carbon content increases with increasing of temperature. It is

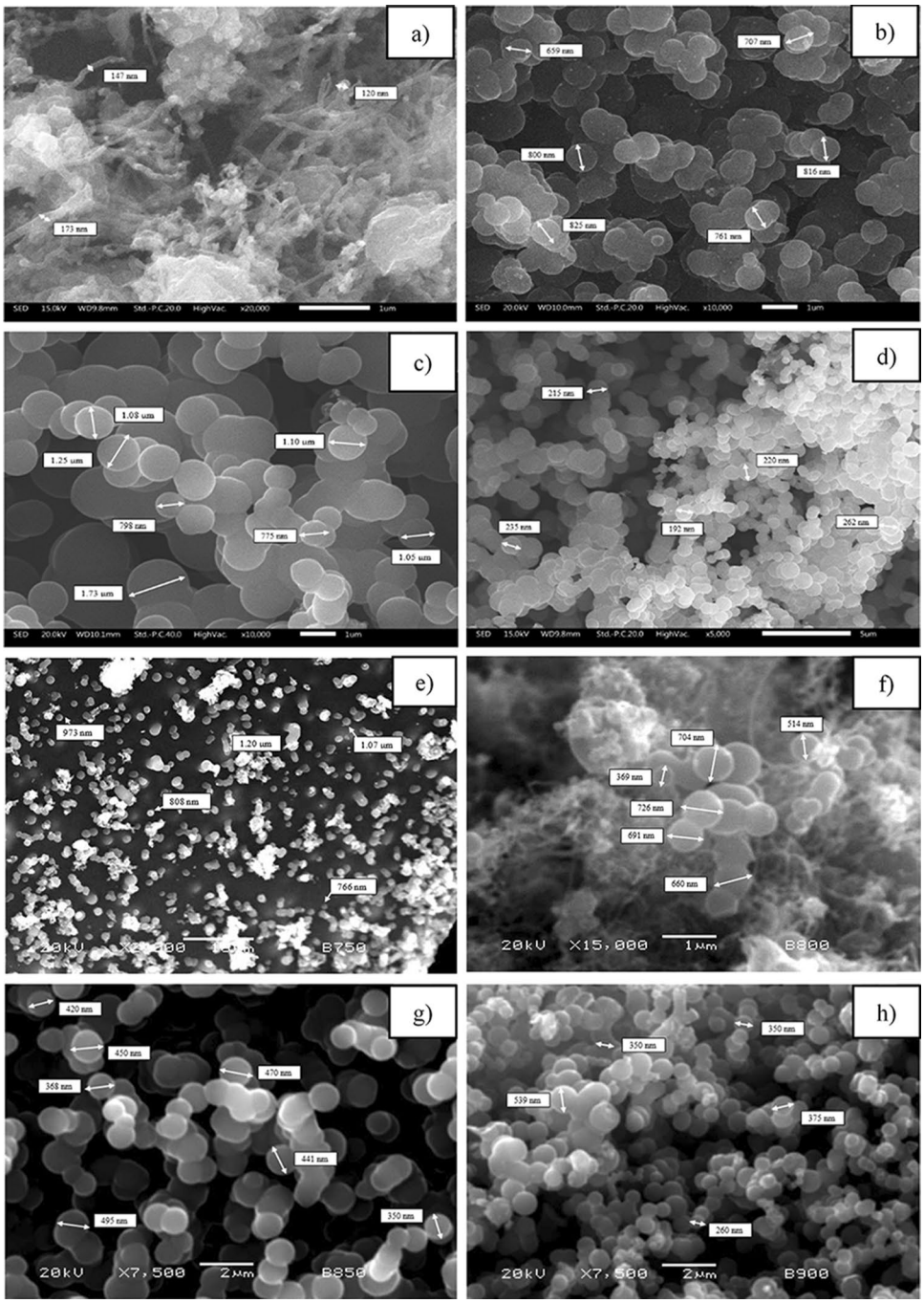

Fig. 1 SEM micrographs of CSs synthesized from the rosin a: **a**, **e** 750 °C, **b**, **f** 800 °C, **c**, **g** 850 °C, and **d**, **h** 900 °C at 30 and 60 min respectively

possible that this occurs because the pyrolysis of rosin is more complete at higher temperatures. García-Ruiz also reported a little increasing of carbon content in synthesis of CNSs from isopropanol and ethyl acetate with raising of temperature [20]. The bigger content of oxygen at the time of 60 min in comparison with 30 min can be due to partial oxidation of CNs as consequence of longer exposition time. Less than 1% atomic of iron and chromium are present in these nanomaterials; it could be due to the catalyst wear during synthesis process.

FTIR detected the functional groups between 400 and 4000 cm^{-1} in all the samples synthesized at different temperatures 750, 800, 850, and 900 °C for 60 and 30 min. Figure 2 shows spectra obtained at 60 min which are typical for both times; a broad band could be observed in the range of 3450–3400 cm^{-1} corresponding to the hydroxyl group (OH) and a weak signal at 2906 cm^{-1} corresponding a CH_x. The bending recorded in the range 1640 cm^{-1} corresponds to the C=O group and around the 1400 cm^{-1} a stretching associated to the C=C group characteristic of spherical and

Table 1 Data from the EDS analysis of the CSs

Temperature/time	Element (at.%)				Total
	Carbon	Oxygen	Chromium	Iron	
750 °C/30 min	98.29	1.68	0.01	0.02	100
800 °C/30 min	98.04	1.91	0	0.04	100
850 °C/30 min	99.75	0.25	0	0	100
900 °C/30 min	99.55	0.39	0.06	0	100
750 °C/60 min	84.31	15.69	0	0	100
800 °C/60 min	89.53	9.37	0.27	0.33	100
850 °C/60 min	89.41	10.54	0.05	0	100
900 °C/60 min	91.83	8.06	0.06	0.06	100

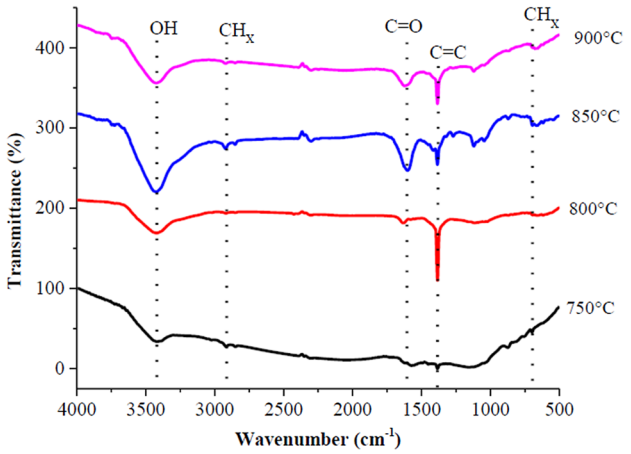

Fig. 2 FTIR analysis of CSs at 60 min

tubular nanostructures is appreciated [21, 22]. The presence of hydroxyl and carbonyl groups can be useful for the enhancement of interaction of carbon spheres with different polymers for composite formation and for usage in vehicle drug delivery and also in other applications. The presence of OH and C=O groups also is proved by EDS analysis, which shows till 15% of oxygen. The functional groups OH, C=O, C=C, and CH_x are also described for CSs obtained at similar conditions by CVD from polynuclear aromatic precursors by Gutierrez-Garcia, who proposed that the intensity and width of their bands indicate that these groups are situated at the edges of CSs [19].

Fig. 3a and Table 2 show Raman analysis in a range of 100 to 3000 cm^{-1} for samples synthesized at 750, 800, 850, and 900 °C/60 and 30 min. D and G bands were observed at all temperatures and synthesis times. D band was found between 1340 and 1360 cm^{-1}, which is attributed to disorder in the graphitic lattice [23]. G band was detected at 1582 and 1600 cm^{-1}, which is related to the degree of graphitization [24]. The high intensity of the G band indirectly shows that there is a high amount of hexagonal carbon in the spherical bodies. The G′ band was recorded in the experiments where the temperature was 850 and 900 °C/60 min and 30 min in the region of 2662 to 2667 cm^{-1}, a band known as D resonance [25]. Studying the ID/IG ratio of the carbon nanostructures synthesized at 750, 800, and 900 °C for 60 and 30 min recorded an ID/IG < 1, suggesting small quantity of defects in the CSs, while in the IG′/IG ratio of the sample at 850 °C at 60 and 30 min was < 1, indirectly supporting that the spherical

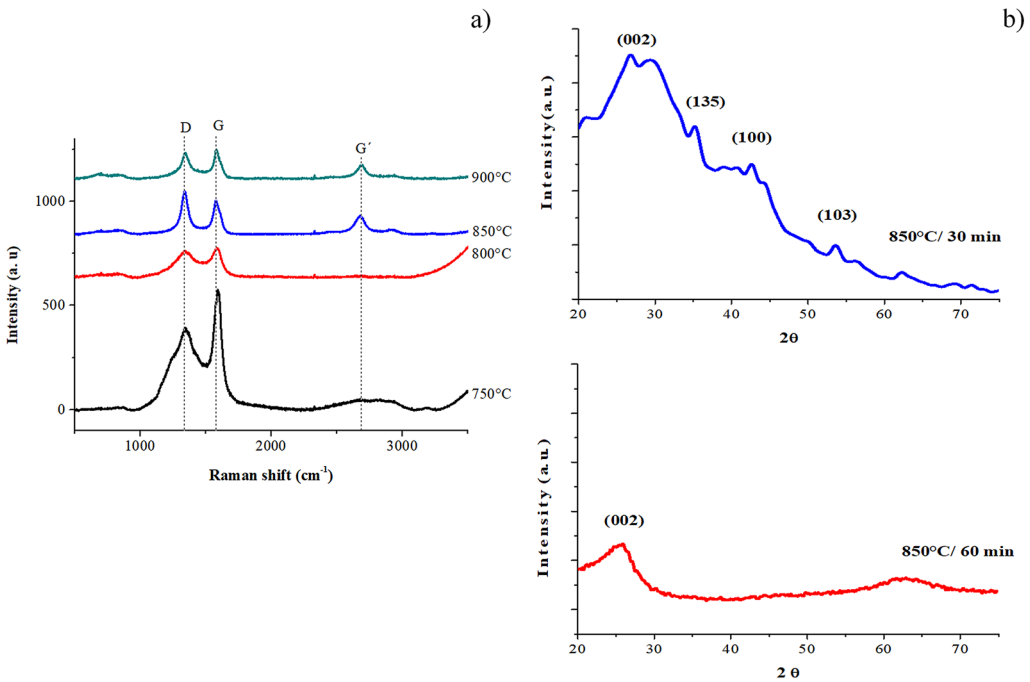

Fig. 3 **a** Raman spectra and **b** XRD diffractograms of CSs

Table 2 Raman spectra data of CNs synthesized for 30 and 60 min

Temperature (°C)	Time (min)	D (cm^{-1})	G (cm^{-1})	G´ (cm^{-1})	ID/IG	IG′/IG
750	30	1329.92	1581.97	–	0.60	–
	60	1354.40	1597.87	–	0.87	–
800	30	1319.14	1592.75	–	0.80	–
	60	1353.92	1583.89	–	0.89	–
850	30	1341.28	1592.75	2687.21	0.91	0.71
	60	1348.61	1579.07	2681.18	1.04	0.87
900	30	1341.28	1592.75	–	0.90	–
	60	1547.17	1598.83	–	0.92	–

bodies are constituted by multilayers graphene sheets [26]. The data of ID/IG in Table 2 shows clearly that the CNSs obtained at 30 min have the minor quantity of defects and as consequence the better degree of graphitization, because at all temperatures the values of relation ID/IG are minor at 30 min than at 60 min.

The XRD diffractogram was run in a software known as March, which compares the diffraction pattern of each sample with a database (patterns) as a reference to identify the phases present. Figure 3b shows the XRD pattern of the CNSs synthesized at 850 °C/30 min and 60 min. The others diffractograms have the similar behavior. A peak at $2\theta = 26.90°$ can be assigned to the (0 0 2) plane corresponding to hexagonal graphitic carbon. Band at $2\theta = 42.83°$ assigned to the (1 0 0) plane corresponds to the hexagonal graphitic lattice characteristic for CSs according to the datasheet JCPDS 96-101-1061 [27–29]. The peaks located at $2\theta = 35.28°$ and 53.39° correspond to the (1 3 5) and (1 0 3), assigned for iron oxide (Fe_3O_4) according to JCPDS 31-0619 [30], which is due to the weathering of the catalyst used in this synthesis (AISI 304 stainless steel bar). It can be observed that the CNSs synthesized at 30 min are more crystalline, than those obtained at 60 min. This fact is confirmed also by Raman data in Table 2, where the ratios ID/IG indicate the mayor degree of graphitization for CNSs synthesized at 30 min for all temperatures. Also, the mayor crystallinity of CNSs obtained at 30-min concur with analysis of data of EDS where the CNSs obtained at 60 min have the percentages of oxygen higher and the percentages of carbon lower, which produces the defects in the crystalline structure. Gutierrez-Garcia also observed (1 0 0) and (0 0 2) planes in carbon spheres obtained from naphthalene and anthracene at the similar conditions but the peaks of CSs obtained from rosin are more definite [19].

Conclusion

In the synthesis of carbon nanomaterials, it is possible to replace petroleum derivatives with renewable, low cost, and readily available green organic precursors, such as coniferous exudates known as rosin. In this research, it was successfully demonstrated that rosin can be effective precursor to synthesize carbon spheres and nanotubes by chemical vapor deposition method with an AISI 304 stainless steel as a catalyst with the possibility to scale the process. The CNSs obtained at all temperatures at 30 min show higher crystallinity and obtained at 60 min have lower crystallinity which was confirmed also by analysis of Raman spectra and EDS. The synthesized CNSs possessed typical functional groups, such as OH, C=O, C=C, and CH_x. The presence of OH and C=O functional groups can be useful for enhancement of interaction of CNSs with different substances, like for vehicle drug delivery and composite materials with polymeric matrix. Also these CNSs can be used for different usage in the nanobiotechnology, electronics, fuel cells, etc.

Acknowledgments CIC of the Universidad Michoacana de San Nicolás de Hidalgo, MICRONA of the Universidad Veracruzana, Tecnológico Nacional México/Instituto Tecnológico de Morelia, ENES UNAM Campus Morelia, and CONACYT México.

Data availability All data generated or analyzed during this study are included in this published article.

Declarations

Conflict of interest We have no conflicts of interest to declare.

References

1. W. Wang, Y. Hou, D. Martinez, D. Kurniawan, W.H. Chiang, P. Bartolo, Polymers (2020). https://doi.org/10.3390/polym12122946
2. J.M. Ambriz-Torres, C.J. Gutiérrez-García, D.L. García-Ruiz, J.J. Contreras-Navarrete, F.G. Granados-Martínez, N. Flores-Ramírez, M.L. Mondragón-Sánchez, L. García-González, L. Zamora-Peredo, O. Hernández-Cristóbal, F. Méndez, L. Domratcheva-Lvova, J. Mater. Sci.: Mater. Electron. (2020). https://doi.org/10.1007/s10854-020-02868-z
3. Y.Z. Jin, C. Gao, W.K. Hsu, Y. Zhu, A. Huczko, M. Bystrzejewski, D.R. Walton, Carbon (2005). https://doi.org/10.1016/j.carbon.2005.03.002

4. A.R.K. Rezaei, Dia Rel Mater. (2018). https://doi.org/10.1016/j.diamond.2018.02.003
5. H.J. Muñoz-Flores, J.H. Ramos, J.T. Sáenz-Reyes, R. Reynoso-Santos, R. Barrera-Ramírez, Rev. Mex de Cie For. (2022). https://doi.org/10.29298/rmcf.v13i73.1188
6. S. Ravi, S. Vadukumpully, J. Environ. Chem. Eng. (2016). https://doi.org/10.1016/j.jece.2015.11.026
7. A.A. Aboul-Enein, A.E. Awadallah, S.M. Solyman, H.A. Ahmed, Fuller. Nanotub. Carbon Nanostruct. (2022). https://doi.org/10.1080/1536383X.2021.2023133
8. P. Anastas, N. Eghbali, Chem. Soc. Rev. (2010). https://doi.org/10.1039/B918763B
9. K. Awasthi, R. Kumar, R.S. Tiwari, O.N. Srivastava, J. Exp. Nanosci. (2010). https://doi.org/10.1080/17458081003664159
10. S.P. Somani, P.R. Somani, M. Tanemura, S.P. Lau, M. Umeno, Curr. Appl. Phys. (2009). https://doi.org/10.1016/j.cap.2008.01.002
11. K. Koziol, B.O. Boskovic, N. Yahya, Carbon Oxide Nanostruct. (2011). https://doi.org/10.1007/8611_2010_12
12. L. Camilli, M. Scarselli, S. Del Gobbo, P. Castrucci, F. Nanni, E. Gautron, S. Leframt, M. De Crescenzi, Carbon (2011). https://doi.org/10.1016/j.carbon.2011.04.014
13. Q.L. Yan, M. Gozin, F.Q. Zhao, A. Cohen, S.P. Pang, Nanoscale (2016). https://doi.org/10.1039/c5nr07855e
14. P. Ghosh, T. Soga, R.A. Afre, T. Jimbo, J. Alloys Compd. (2008). https://doi.org/10.1016/j.jallcom.2007.08.027
15. M. Inagaki, Carbon **35**, 711 (1997)
16. R. Li, A. Shahbazi, Trends Renew. Energy (2015). https://doi.org/10.17737/tre.2015.1.1.009
17. J.M. Ambriz-Torres, L.D. Lvova, C.J. García, P. Garnica-González, O. Aguilar-García, J.J. Contreras-Navarrete, MRS Adv. (2022). https://doi.org/10.1557/s43580-022-00338-8
18. J.A. Guzmán-Fuentes, J.J. Contreras-Navarrete, E. Cadenas-Calderón, J.M. Ambriz-Torres, D.L. García-Ruíz, C.J. Gutiérrez-García, L. Domratcheva-Lvova, MRS Adv. (2020). https://doi.org/10.1557/adv.2020.399
19. C.J. Gutiérrez-García, J.M. Ambriz-Torres, J.J. Contreras-Navarrete, F.G. Granados-Martínez, D.L. García-Ruiz, L. García-González, L. Domratcheva-Lvova, Physica E (2019). https://doi.org/10.1016/j.physe.2019.04.007
20. D.L. García-Ruiz, F.G. Granados-Martínez, C.J. Gutiérrez-García, J.M. Ambriz-Torres, J.J. Contreras-Navarrete, N. Flores-Ramírez, L. Domratcheva-Lvova, Rev. Mex. Ing. Quí. (2019). https://doi.org/10.24275/uam/izt/dcbi/revmexingquim/2019v18n2/GarciaR
21. K.R. Gbashi, Iraqi J. Phys. (2017). https://doi.org/10.30723/ijp.v15i35.55
22. K. Saxena, P. Kumar, V.K. Jain, New Carbon Mater. (2011). https://doi.org/10.1016/S1872-5805(11)60088-7
23. E.F. Antunes, A.O. Lobo, E.J. Corat, V.J. Trava-Airoldi, Carbon (2007). https://doi.org/10.1016/j.carbon.2007.01.003
24. M.A. Ermakova, D.Y. Ermakov, A.L. Chuvilin, G.G. Kuvshinov, J. Catal. (2001). https://doi.org/10.1006/jcat.2001.3243
25. M.S. Dresselhaus, G. Dresselhaus, R. Saito, A. Jorio, Phys. Rep. (2005). https://doi.org/10.1016/j.physrep.2004.10.006
26. L.G. Cançado, K. Takai, T. Enoki, M. Endo, Y.A. Kim, H. Mizusaki, A. Jorio, L.N. Coelho, R. Magalhães-Paniago, M.A. Pimenta, Appl. Phys. Lett. (2006). https://doi.org/10.1063/1.2196057
27. R.W. Wyckoff, Cryst. Struct. **1**, 7 (1963)
28. J. Fayos, J. Solid State Chem. (1999). https://doi.org/10.1006/jssc.1999.8448
29. A.N. Mohan, B. Manoj, Int. J. Electrochem. Sci. **7**, 9537 (2012)
30. G.C. Allen, K.R. Hallam, J.A. Jutson, Powder Diffr. (1995). https://doi.org/10.1017/S0885715600014779